Review

Recent Progress and Challenges of Metal-Organic Framework-Based Membranes for Gas Separation

Shunsuke Tanaka *, Kojiro Fuku, Naoki Ikenaga, Maha Sharaf, Keizo Nakagawa

Posted Date: 29 December 2023

doi: 10.20944/preprints202312.2107.v1

Keywords: metal-organic frameworks; polycrystalline membranes; membrane formation; intergrowth; grain boundary voids; adsorption; diffusion; gas separation

Review

Recent Progress and Challenges of Metal-Organic Framework-Based Membranes for Gas Separation

Shunsuke Tanaka [1,2,3,*], Kojiro Fuku [1,2,3], Naoki Ikenaga [1,2,3], Maha Sharaf [4] and Keizo Nakagawa [5,6]

[1] Department of Chemical, Energy and Environmental Engineering, Faculty of Environmental and Urban Engineering, Kansai University, 3-3-35 Yamate-cho, Suita-shi, Osaka 564-8680, Japan; k.fuku@kansai-u.ac.jp (K.F.); ikenaga@kansai-u.ac.jp (N.I.);
[2] Organization for Research and Development of Innovative Science and Technology (ORDIST), Kansai University, 3-3-35 Yamate-cho, Suita-shi, Osaka 564-8680, Japan
[3] Carbon Neutrality Research Center (CNRC), Kansai University, 3-3-35 Yamate-cho, Suita-shi, Osaka 564-8680, Japan
[4] Reactor Materials Department, Nuclear Materials Authority, POB 530, El Maadi, Cairo 11728, Egypt; maha_sharaf7@yahoo.com
[5] Graduate School of Science Technology and Innovation, Kobe University, 1-1 Rokkodai, Nada, Kobe 657-8501, Japan; k.nakagawa@port.kobe-u.ac.jp
[6] Research Center for Membrane and Film Technology, Kobe University, 1-1 Rokkodai, Nada, Kobe 657-8501, Japan
* Correspondence: shun_tnk@kansai-u.ac.jp; Tel.: +81-6-6368-0851

Abstract: Metal-organic frameworks (MOFs) represent the largest class of materials among the crystalline porous materials ever developed and have attracted attention as core materials for separation technology. Their extremely uniform pore aperture and nearly unlimited structural and chemical characteristics have attracted great interest and promise in applying MOFs to adsorptive and membrane–based separations. This paper reviews the recent research and development of MOF membranes for gas separation. Strategies for polycrystalline membranes and mixed matrix membranes are discussed, with a focus on separation systems involving hydrocarbon separation and CO_2 capture. Challenges and opportunities for the industrial deployment of MOF membranes are also be discussed, providing guidance for the design and fabrication of future high-performance membranes. The contributions of the underlying mechanism to separation performances, and the adopted strategies and membrane processing technologies for breaking the selectivity/permeability trade–off are discussed.

Keywords: metal-organic frameworks; polycrystalline membranes; membrane formation; intergrowth; grain boundary voids; adsorption; diffusion; gas separation

1. Introduction

Research, development and demonstration tests for the practical application of metal-organic frameworks (MOFs) are underway involving companies and universities in various fields [1–5]. MOFs are porous materials consisting of coordination bonds between metal ions and multifunctional organic ligands, which can exhibit unparalleled properties and functions (e.g., storage, adsorption, separation, catalytic, electromagnetic, and optical properties by tuning their framework composition and pore structure. As companies begin to produce and market MOFs, products are being created that exploit their properties. Queen's University Belfast start-ups MOF Technologies and DECCO have applied MOFs to a product that keeps fruit and vegetables fresh [6]. The role of MOFs is to store and release 1-methylcyclopropene, which inhibits the action of ethylene that ripens fruit and vegetables, as required. NuMat Technologies, a start-up company from Northwestern University, has commercialized MOFs as a gas cylinder that can store and safely transport toxic gases for the semiconductor industry [7]. Atomis, a start-up company from Kyoto University, is in the process of gaining approval for commercial use of MOF-based high-pressure gas container, CubiTan®.

 doi:10.20944/preprints202312.2107.v1

SyncMOF, a start-up company from Nagoya University, is in the process of commercializing MOF-based gas separation systems, MOFclean. Transaera, a start-up company from Massachusetts Institute of Technology, is in the process of commercializing dehumidifying air conditioning systems using MOFs. Svante and Crimeworks are also piloting the application of MOFs in direct air capture, which captures CO_2 directly from the atmosphere. Thus, large-scale applications of MOFs are expected to expand.

2. Characteristics of MOFs

2.1. Structural Flexibility

Some MOFs have flexible pore structures. It is known that the pore structure changes when gas is adsorbed. Some of these MOFs exhibit unique adsorption behavior in that they behave as nonporous materials under low gas pressure conditions and show no adsorption performance. On the other hand, when the gas pressure reaches a certain threshold pressure (so-called gate-opening pressure), they change to a porous structure, resulting in a rapid increase in adsorption. The gate-opening type adsorption behavior, which is not observed in conventional porous materials, depends on the combination of metal ions and ligands constituting the framework. Various types of structural flexibility have been reported [8]. For example, (1) changes in pore shape from a rhombic structure to a square structure and vice versa, (2) changes in the relative position of interpenetrating structures, (3) stretching and shrinking of lattice layers, and (4) rotation of ligands at the pore aperture. and is caused by various factors, such as the pore shape changing from a rhombic structure to a square structure or vice versa, the relative position of interpenetrating structures changing, the lattice layers expanding and contracting, and ligand rotation at the pore aperture, and so on. Furthermore, adsorption behavior has been reported to vary with crystal size and shape. For example, $[Cu_2(bdc)_2(bpy)]n$ (bdc = benzene-1,4-dicarboxylic acid, bpy = 4,4'-dipyridyl) [9] and ZIF-8 [10] have been reported to exhibit higher gate-opening pressure with smaller crystals.

2.2. Structural Stability

Thermal and chemical stability of materials is one of the most important properties for not only membrane separation but also for many industrial applications. Due to the instability of the metal-ligand coordination bond, the structure of many MOFs is degraded by moisture in the air. In order to prevent the collapse of the network structure due to hydrolysis reactions of the metal-ligand coordination bonds or ligand substitution reactions, it is effective to have either a strong coordination bond that is thermodynamically stable or a kinetically stable structure using large steric hindrance. Basically, when the coordination environment with the ligand is the same, metal ions with higher valence and charge density form a more stable framework. This tendency is explained according to the HSAB theory and supported by many findings in MOF studies [11]. According to the HSAB theory, carboxylic acid ligands can be regarded as hard bases that form stable complexes with hard acid metal ions such as Al^{3+}, Cr^{3+}, Fe^{3+}, Ti^{4+}, and Zr^{4+}. MIL series and UiO-66 are well-known MOFs with high structural stability synthesized by such a combination (Figure 1). Imidazolate and azolate ligands of soft bases form relatively stable structures together with divalent metal ions of soft acids such as Zn^{2+}, Co^{2+}, and Cu^{2+}. The most representative example is ZIF series, which is composed of Zn^{2+} and imidazolate [12].

Preprints (www.preprints.org) | NOT PEER-REVIEWED | Posted: 29 December 2023 doi:10.20944/preprints202312.2107.v1

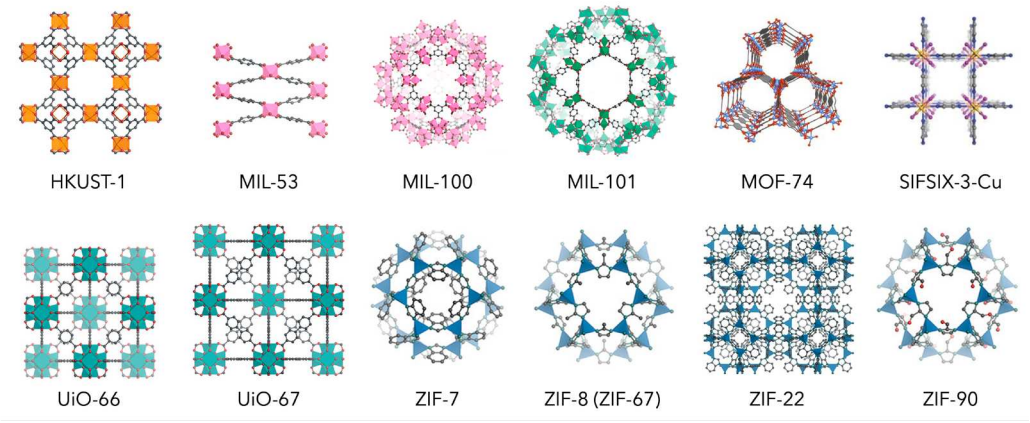

Figure 1. Representative MOF structures.

3. Hydrocarbon Adsorption on MOFs

3.1. Olefins and Paraffins

The first MOF investigated for potential application to olefin/paraffin separation was HKUST-1, which consists of a paddle-wheel Cu(II) dimer and 1,3,5-benzenetricarboxylate as building blocks. Wang et al. measured the adsorption isotherms of C_2H_4 and C_2H_6 on HKUST-1 at 295 K and showed that C_2H_4 is preferentially adsorbed [13]. Water molecules are coordinated to the metal site of HKUST-1 and dehydration forms coordinatively unsaturated open metal sites [14]. Lamia et al. found that C_2H_4 is adsorbed due to the interaction between the π-electrons of C_2H_4 and the partially positively charged open metal site, whereas C_2H_6, which has no C=C double bond, has a low binding affinity to the open metal site, resulting in a selective separation function [15].

MOFs with open metal sites include the MIL series such as MIL-53, MIL-96 and MIL-100 and MOF-74. The MIL series, consisting of trivalent transition metals such as Fe(III), Cr(III), Al(III) and V(III), has been widely studied as MOFs for gas separation. Compared to divalent metals, trivalent transition metals have stronger bonds to ligands and can form more chemically stable structures [16]. However, the strong bonding between the metal and the ligand makes it difficult to synthesize MOFs with high crystallinity, and synthetic methods that satisfy the conditions for spontaneous self-assembly by reversible "weak bonding" are required. For example, MOFs have been synthesized under strongly acidic conditions using HF or HCl [17–20] or by a solvothermal method at high temperatures (100~ °C) [21–23].

The MIL series has trivalent metal sites with high electrophilicity and is excellent for adsorption of electron-rich olefins. Yoon et al. reported that MIL-100(Fe) can be applied to C_3H_6/C_3H_8 separation [24]. Lee et al. reported that MIL-101(Cr), from which terephthalate anions were removed by treatment with NH_4F solution, showed C_2H_4/C_2H_6 selectivity ~4 [25]. In addition, attempts to improve the selectivity by using the interaction between Cu(I) or Ag(I) sites and C=C bonds of C_2H_4 have been reported by depositing Cu nanoparticles on the pore surface of MIL-101(Cr) [26] or by introducing a functional group -SO_3Ag as a building block ligand [27]. Similarly, Kim et al. obtained C_3H_6/C_3H_8 selectivity ~13 by modifying MIL-100(Fe) with Cu(I) [28].

MOF-74 is a honeycomb structure composed of Mg(II), Mn(II), Ni(II), Co(II), Zn(II), Cu(II) or Fe(II) and 2,5-dihydroxyterephthalate as building blocks. Bao et al. first investigated Mg-MOF-74 for the separation of C_2H_4/C_2H_6 and C_3H_6/C_3H_8 (Figure 2) [29]. Bae et al. compared the influence of metal sites on the adsorption selectivity of C_3H_6/C_3H_8 using Mg-, Mn-, and Co-MOF-74. The effect of metal sites on the adsorption selectivity of C_3H_6/C_3H_8 was compared, and it was reported that the selectivity was higher for Mg (selectivity 4.5) < Mn (24) < Co (46) [30]. The influence of the type of phthalate ligand of MOF-74 on the olefin/paraffin separation was also studied, and the replacement of 2,5-dihydroxyterephthalate with 4,6-dihydroxyisophthalate resulted in higher C_2H_4/C_2H_6 (>259 and C_3H_6/C_3H_8 selectivity (>55) of Fe-MOF-74 [31].

Preprints (www.preprints.org) | NOT PEER-REVIEWED | Posted: 29 December 2023 doi:10.20944/preprints202312.2107.v1

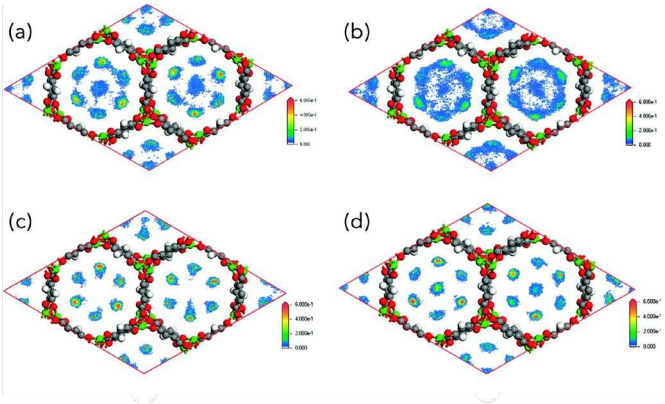

Figure 2. Equilibrium snapshots of (**a**) C_2H_6, (**b**) C_2H_4, (**c**) C_3H_8, and (**d**) C_3H_6 in Mg-MOF-74 at 1 bar. All adsorbates were preferentially adsorbed by the open metal sites and each metal can adsorb one molecule. Reprinted with permission from ref. [29]. Copyright 2011 American Chemical Society.

Olefin selective adsorption using open metal sites of MOFs is enhanced by increasing the charge density of coordinatively unsaturated open metal sites. However, these MOFs exhibit very high enthalpies of adsorption (> tens of kJ/mol) and suffer a significant energy penalty in adsorbent regeneration. Furthermore, such MOFs may decrease the adsorption capacity in the presence of water.

Most MOFs without open metal sites do not show selective adsorption of olefins/paraffins, with the notable exception of NOTT-300, which is composed of $[AlO_4(OH)_2]$ and biphenyl-3,3',5,5'-tetracarboxylate as building blocks. NOTT-300 exhibits a very high C_2H_4/C_2H_6 selectivity of 48.7, while its low enthalpy of adsorption, approximately 16 kJ/mol, reduces the energy penalty for regeneration. The energy penalty for regeneration is also reduced [32].

The use of adsorbents that selectively adsorb paraffins saves energy by eliminating the adsorption-desorption cycle required for olefin recovery. However, C_2H_6 has a smaller quadrupole moment and larger dynamic molecular size than C_2H_4, making selective adsorption generally more difficult. On the other hand, selective adsorption of C_2H_6 has been reported in several MOFs. ZIF-7, composed of Zn(II) and benzimidazolate, has been reported to adsorb C_2H_6 (and C_3H_8 compared to C_3H_6) at lower pressures than C_2H_4, although there is no large difference in saturation adsorption capacity for olefins and paraffins [33,34].

MAF-49, which is composed of Zn(II) and the triazole ligand bis(5-amino-1H-1,2,4-triazol-3-yl)methane and has one-dimensional zigzag channels, is also known to preferentially adsorb C_2H_6 [35]. The enthalpy of C_2H_6 adsorption by MAF-49 (60 kJ/mol) is higher than that of C_2H_4 (48 kJ/mol), and it preferentially adsorbs C_2H_6 in the low-pressure region, where C-H···N hydrogen bonds and electrostatic interactions occur between electronegative nitrogen atoms and C_2H_6 (Figure 3). On the other hand, for C_2H_4, it was concluded that steric hindrance and electrostatic repulsion occur between the C-H of C_2H_4 and the methylene group of the ligand. Therefore, the placement of multiple polar functional groups at appropriate positions in the framework may be effective in achieving the desired selective separation.

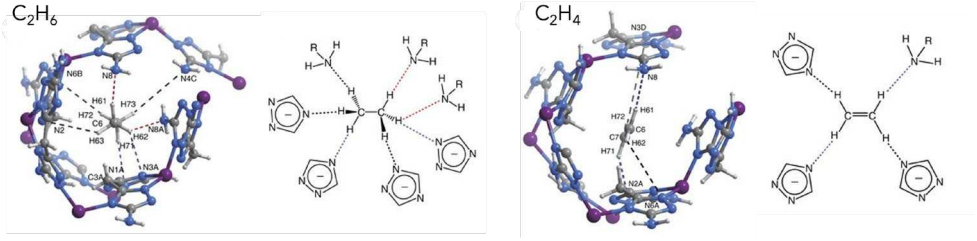

Figure 3. Preferential adsorption sites and host-guest interactions for C_2H_6 and C_2H_4 in MAF-49. Reproduced from ref. [35] with permission. Copyright 2015 Springer Nature.

 doi:10.20944/preprints202312.2107.v1

3.2. Other Hydrocarbons

Separation of 1,3-butadiene from C4 hydrocarbon mixtures is essential to produce synthetic rubber. However, the C4 isomers have close boiling points, and some components form azeotropic mixtures. Kishida et al. discussed the possibility of separating 1,3-butadiene from C4 hydrocarbons by MOF [36]. The synthesized MOF is called SD-65 and has an interpenetrating structure in which Zn(II) is coordinated to two components, 5-nitroisophthalate and 1,2-di(4-pyridyl)ethylene. SD-65 adsorbed almost no *n*-C_4H_{10}, *i*-C_4H_{10}, 1-butene, isobutene, trans-2-butene and cis-2-butene (adsorption capacity ~2.5 cm^3/g at approximately 1 bar), while it adsorbed 40 cm^3/g of 1,3-butadiene. The pore structure remains closed until the pressure of 1,3-butadiene is about 0.6 bar, at which point the pore structure rapidly transitions to an open pore structure and butadiene is adsorbed. Other MOFs have been investigated for 1,3-butadiene separation, all of which have potential, but there are still many issues to be solved to meet the separation selectivity requirements [36–40].

Separation of linear/branched hydrocarbons using MOFs has also been studied. Pan et al. reported that MOF composed of paddlewheel Cu(II) dimer and 4,4'-(hexafluoroisopropylidene)bis-(benzoic acid) adsorbs C_3H_8, C_3H_6 and *n*-C_4H_{10}, while *i*-C_4H_{10}, *n*-pentane, *i*-pentane, *n*-Hexane and 3-methylpentane are not adsorbed [41]. Peralta et al. reported the separation of linear/branched hydrocarbons by ZIF-8 [42]. ZIF-8 adsorbs *n*-hexane, and 3-methylpentane, but not 2,2-dimethylbutane.

The MIL series, including MIL-47 and MIL-53, has also been studied for xylene isomer separation [43–47]. MIL-47 and MIL-53 have the same crystal topology consisting of $[MO_4(OH)_2]$ and phthalic acid. MIL-47, which is composed of V(III) has a rigid structure, whereas MIL-53, which is composed of Al(III), Cr(III) and Fe(III), shows a unique flexibility called the breathing effect. The *p*-xylene/*m*-xylene separation by MIL-47 showed a selectivity of 2.9. On the other hand, MIL-53(Al) could not separate *p*-xylene and *m*-xylene.

UiO-66, composed of zirconium and terephthalic acid, is well-known for its excellent chemical and thermal stability. UiO-66 preferentially adsorbs branched hydrocarbons, 2,2-dimethylbutane and 2,3-dimethylbutane, over linear hydrocarbons, *n*-hexane [48]. This unique adsorption behavior is attributed to the 6-7 Å triangular lattice of the channel pores of UiO-66, which is believed to be responsible for the preferential adsorption of *o*-xylene over *p*-xylene.

4. CO_2 Separation and Capture

Since global CO_2 emissions from energy conversion such as power generation account for more than 40% of total global CO_2 emissions, decarbonization of energy conversion is crucial to reducing emissions. CO_2 separation and capture processes in the power generation sector can be classified into pre-combustion, post-combustion, and oxy-fuel combustion. The most mature technology for capturing CO_2 after combustion is chemical absorption using monoethanolamine (MEA). However, the energy cost of CO_2 separation and capture is high, even for power plants that use the captured CO_2 for enhanced oil recovery (EOR) [49]. Carbon pricing through "carbon taxes" and "emissions trading" has been introduced as a measure to reduce CO_2 emissions. The cap-and-trade European Union Emissions Trading Scheme (EU-ETS) has become the most recognized carbon market in the world, with the EU-ETS price exceeding 50€/t-CO_2 in May 2021. Many international organizations, including the International Energy Agency (IEA) and the International Renewable Energy Agency (IRENA), have stated that carbon pricing will spur innovation in low-carbon technologies and increase the potential for new technologies to replace existing technologies [50]. Membrane separation is considered a promising next-generation separation technology because it can operate continuously (no need to regenerate separators), consumes less energy than other separation methods, and can be easily integrated into existing technologies due to its compact equipment [51]. Membrane gas separation was commercialized in the late 1970s for hydrogen separation and has since been applied to carbon dioxide separation from natural gas, biogas, and landfill gas, air separation (nitrogen-enriched gas and oxygen-enriched gas production), and air dehumidification. However, membrane separation as a CO_2 separation and recovery technology for CO_2 Capture, Utilization and Storage (CCUS) has only been studied up to bench scale with a few exceptions.

 doi:10.20944/preprints202312.2107.v1

Polymers such as silicone rubber, cellulose acetate, polysulfone, and polyimide have been mainly used as membrane materials. Recently, porous membranes with sub-nanometer sized pores have been extensively studied, with silica and zeolite membranes receiving much attention. Mixed matrix membranes (MMMs), in which MOFs are mixed with polymer matrix as filler, have also been actively studied. Pre-combustion is primarily intended for use in integrated gasification combined cycle (IGCC), a process in which coal and natural gas are partially oxidized to produce natural gas vapor. Fuel gas is purified by separating and recovering CO_2 from synthesis gas (consisting primarily of H_2 and CO) produced by partial oxidation of coal and natural gas or by steam reforming of natural gas to produce H_2 and CO_2 by reacting CO with aqueous gas shift. Since high-pressure gas is the separation target (mainly CO_2/H_2) in pre-combustion, equipment such as vacuum pumps are not required, saving energy and cost. However, the separation membrane must be durable under high temperature and high pressure. In addition, since H_2 has a smaller molecular size than CO_2, H_2 selective permeation membranes have been mainly studied. On the other hand, post-conversion targets the separation of combustion exhaust gas generated from boilers in power plants at relatively low pressure, which requires the installation of vacuum pumps and compressors, making it difficult to achieve significant energy conservation and cost reduction compared to existing technologies. For energy conservation and cost reduction, high permeability is required for separation membranes from the viewpoint of reducing the required membrane area.

5. MOF-Based Membranes

5.1. Types of Membranes

Separation membranes based on MOF can be broadly classified into two categories. One is a polycrystalline membrane composed of MOF alone, and the other is a mixed matrix membrane (MMM) in which MOF is mixed with a polymer membrane as a filler. Similar to porous inorganic membranes such as silica and zeolite membranes, MOF polycrystalline membranes are often formed on porous ceramic supports to ensure the mechanical strength of the membrane. MOFs are often compared and discussed with zeolites because of their similarities with zeolites in terms of crystalline porous structure. MMM, on the other hand, is a strategy to improve membrane performance by synergistically combining the excellent processability of polymers with the porous properties of MOF fillers.

MOF polycrystalline membranes exhibit high separation performance by selecting the optimum structure for the separation target because the only membrane permeation pathway for gas molecules is through the pores of the MOFs. However, nonselective permeation often occurs due to the formation of grain boundaries between crystals, pinholes, and intracrystalline defects. In order to fabricate membranes with dense grain boundaries, polycrystalline membranes are generally prepared by using seed crystals via secondary growth method [52–55]. Although pioneering studies of MOF membrane formation reported in the late 2000s did not lead to the reporting of gas permeation results, these studies stimulated research on polycrystalline MOF membranes and various membrane preparation methods have been reported.

MMM is a membrane in which MOF fillers are dispersed in a polymer matrix. The dispersion state of the polymer and filler greatly affects the performance of the membrane [56]. MMMs may be prepared on supports, but they differ from MOF polycrystalline membranes in that the processability of polymers can be used to fabricate freestanding membranes. Since MOFs contains organic ligands, it is expected to interact well with the polymer matrix and inhibit microvoid formation between filler/polymer. The use of highly porous MOFs as fillers is expected to improve membrane permeability. However, to improve permeability, it is necessary to increase the MOF filler content. However, as filler content increases, mechanical properties and processability of polymers decrease. In general, the smaller the fillers, the more likely they are to aggregate. If interface defects are formed in the MMM due to non-uniform dispersion caused by aggregation of fillers and/or poor interaction between filler and polymer, gas molecules will preferentially diffuse through the defects and separation performance will be degraded. In order to suppress filler agglomeration and poor

Preprints (www.preprints.org) | NOT PEER-REVIEWED | Posted: 29 December 2023 doi:10.20944/preprints202312.2107.v1

dispersion in the polymer matrix, a technique to control the filler/polymer heterointerface at the molecular level is required.

5.2. MOF Membrane Preparation Method and Points to Consider

If MOFs can be thinned so that there are no voids between crystals, they can be applied as separation membranes. However, fabricating polycrystalline membranes is not so easy. It must be noted that cracks, pinholes, and intra-crystal defects between crystals cause non-selective permeation, and that large areas must be achieved with thin membranes. Various methods have been proposed for preparing MOF membranes (Figure 4).

To fabricate continuous polycrystalline membranes on a support, a dense heterogeneous nucleation field must exist on the support surface. The secondary growth method is often used, in which pre-prepared seed crystals are loaded on the support surface and grown to form continuous films. Seeding techniques such as dip coating [57], slip coating [58] and rubbing [59] are used, followed by solvothermal or hydrothermal synthesis. In general, it is important to uniformly load seed crystals on support surface, and to make thin membranes (<1 μm), seed crystals of about 100 nm are required to allow sufficient crystal intergrowth [60]. The secondary growth method is an effective way to promote the formation of dense heterogeneous nuclei, which is important for thin membrane growth, but it still poses a challenge in terms of adhesion between membrane and support.

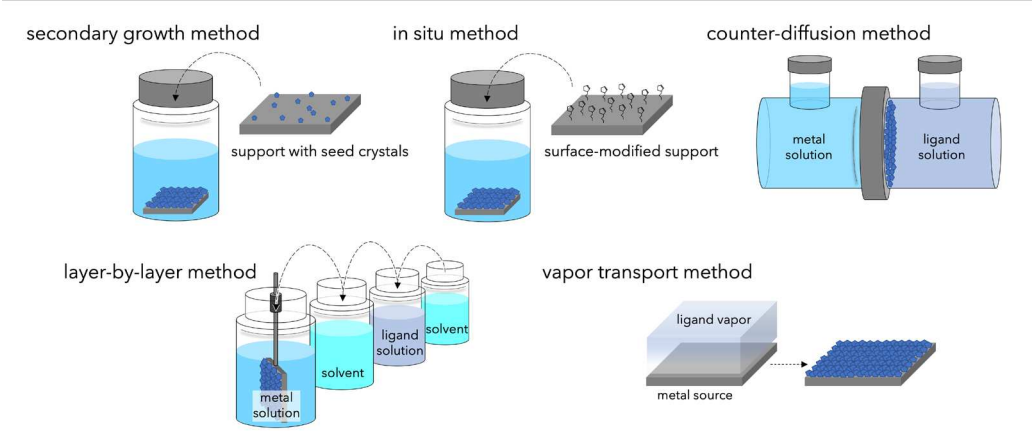

Figure 4. Schematic of the methods developed for synthesis of continuous MOF membranes.

To address the issue of adhesion between membrane and support, modification of the support surface with compounds that bind the MOF crystals and the support has been used [61–64]. These compounds have one end that can coordinate with the nodes constituting the MOF and the other end that can covalently bond with the support. The functional groups immobilized on the support cause heterogeneous nucleation of MOFs and promote crystal growth, resulting in continuous MOF membranes with a high degree of crystallinity and relatively thin membrane thickness. The chemical modification method is also effective when using polymers as supports in addition to ceramic supports [65,66].

Another method has been proposed to solve the problem of adhesion between the membrane and the support by growing and immobilizing MOFs in the pores of the porous support. The counter-diffusion method is used to deposit MOFs in the pores of the support [67–69]. In the counter-diffusion method, the solutions of metal ions and organic ligands are supplied from opposite sides of the support, and the MOF layer is formed at the interface where the diffusing raw materials come into contact by chemical potential gradient.

Grain boundary defects are one of the most important problems in continuous polycrystalline membranes. The difference in the coefficient of thermal expansion between MOF crystals and support is a source of stress and causes defects in the membrane. Membrane defects can also occur during the activation process of MOF. ZIF-78 membrane synthesized using *N*,*N*-dimethylformamide as the reaction solvent easily forms membrane defects when activated at 100°C under vacuum [70].

Preprints (www.preprints.org) | NOT PEER-REVIEWED | Posted: 29 December 2023 doi:10.20944/preprints202312.2107.v1

Therefore, it is effective to bring the coefficients of thermal expansion of the two materials closer, but such a combination is not always possible. On the other hand, it has been demonstrated that membrane defects can be reduced by optimizing the cooling rate after membrane formation at high temperature [71]. To solve this problem, it is effective to replace the remaining reaction solvent with a solvent with low boiling point and surface tension, such as methanol or ethanol, before heating MOF under vacuum. In addition, various post-synthetic modifications have been investigated to suppress the generation of membrane defects and to repair defects that have occurred.

5.3. Olefin/Paraffin Separation

MOFs have potential for a wide range of separation targets due to their excellent pore structure and composition, as well as the diversity of their synthesis and membrane production methods. Although MOFs appear promising for olefin/paraffin separation, only a few MOF membranes are currently available. While they have been demonstrated to be effective for the separation of C_3H_6/C_3H_8, few have been reported to be able to efficiently separate C_2H_4/C_2H_6.

ZIF-8, which is composed of Zn(II) and 2-methylimidazolate as building blocks and has a SOD structure, has been the most studied for C_3H_6/C_3H_8 separation. The effective pore size of ZIF-8 is 4.0-4.2 Å, but even 1,2,4-trimethylbenzene of approximately 7.6 Å enters the pores [72], suggesting a lack of sharp molecular sieving. Indeed, the selectivity of CO_2/CH_4 separation by the ZIF-8 membrane is only about 5 [73]. On the other hand, the structural flexibility of ZIF-8 works effectively in C_3H_6/C_3H_8 separation, showing a sharp cut-off between C_3H_6 and C_3H_8 molecular sizes. The diffusion selectivity of C_3H_6/C_3H_8 in ZIF-8 is theoretically estimated to be approximately 125 [74], and various studies on ZIF-8 membranes have been conducted with this value as a benchmark. Pan et al. first reported the separation of C2/C3 hydrocarbons (C_2H_6/C_3H_8, C_2H_4/C_3H_6 and C_2H_4/C_3H_8) using a ZIF-8 membrane prepared on a porous alumina disc [75]. Meanwhile, at the same time, Bux et al. reported a selectivity of only 2.8 for C_2H_4/C_2H_6 separation [76]. Subsequently, intensive research on ZIF-8 membranes was undertaken after Zhang et al. showed that the pore size of ZIF-8 was effective for C_3H_6/C_3H_8 separation by estimating the diffusion coefficient [77] (Table 1). Various improvements have been made to meet the separation performance requirements, such as optimizing secondary growth and activation conditions, and devising unique membrane preparation methods.

Table 1. C_3H_6/C_3H_8 separation performance of ZIF-8 membranes described in this review.

Method	Support	Membrane Thickness	Q_{C3H6} (mol m^{-2} s^{-1} Pa^{-1})	$\alpha_{C3H6/C3H8}$	Ref.
secondary growth	α-Al_2O_3	~1 μm	8.1×10^{-9}	90.2	[60]
in situ	α-Al_2O_3	1 μm	8.5×10^{-9}	36	[64]
counter-diffusion	α-Al_2O_3	~1.5 μm	2.1×10^{-8}	50	[68]
counter-diffusion	α-Al_2O_3	~80 μm	2.3×10^{-8}	57	[69]
IMMP	Torlon®	8.8 μm	1.3×10^{-8}	12	[78]
IMMP	Torlon®	8.1 μm	1.5×10^{-8}	180	[79]
heteroepitaxial	α-Al_2O_3	1.0 μm	3.7×10^{-8}	209.1	[80]
FCDS	Pt coated AAO	~200 nm	1.7×10^{-8}	304.8	[81]
GVD	PVDF	114 nm	2.1×10^{-7}	67.8	[82]
ALD	γ-Al_2O_3	~500 nm	8.8×10^{-8}	71	[83]

Brown et al. devised an interfacial microfluidic membrane processing (IMMP) method to fabricate ZIF-8 membranes on polyamide-imide hollow fibers (Torlon®) [78]. In the IMMP method, an aqueous solution of 2-methylimidazole is fed to one side of the hollow fiber and a 1-octanol solution of zinc nitrate is continuously fed to the opposite side for counter-diffusion to form ZIF-8 membrane at an incompatible interface. This method is promising for scale-up and mass production of membranes, as it is low-cost and can process several hollow fibers with high specific surface area simultaneously. In their initial report, the C_3H_6/C_3H_8 selectivity was only 12 due to the presence of membrane defects. Thereafter, the C_3H_6/C_3H_8 selectivity reached 180 (at a feed gas pressure of 1 bar)

Preprints (www.preprints.org) | NOT PEER-REVIEWED | Posted: 29 December 2023 doi:10.20944/preprints202312.2107.v1

[79] by controlling the membrane formation and optimizing the membrane growth process and the microstructure of the hollow fibers. It was also confirmed that the selectivity of 90 was maintained even when the feed gas pressure was 9.5 bar.

Besides controlling the microstructure between neighboring crystals, it is also important to control the structural flexibility of MOFs to improve the separation selectivity of polycrystalline membranes. For ZIFs, the framework flexibility caused by the rotation of the ligands allows larger molecules to permeate, resulting in reduced molecular sieving effect. In contrast, Tanaka et al. showed that the structural flexibility of ZIF-8 varies depending on the crystal size [10] and proposed that the membrane performance can be tuned by the size of the primary particles constituting the polycrystalline membrane [64]. On the other hand, the kinetic properties of the ZIF ligand are altered by substituting the metal nodes. ZIF-67 has the same crystal topology as ZIF-8, with Co(II) as a node instead of Zn. It is known that the bonding of Co(II)-2-methylimidazolate is stronger than that of Zn(II)-2-methylimidazolate, which makes ZIF-67 more rigid than ZIF-8 and limits the rotation of the ligand. Kwon et al. grew ZIF-67 heteroepitaxially on a ZIF-8 seed layer and then ZIF-8 on a ZIF-67 layer to prepare a membrane with a trilayer ZIF-8/ZIF-67/ZIF-8 structure (Figure 5) and demonstrated that extremely high C_3H_6/C_3H_8 selectivity is achieved [80]. Zhou et al. devised a fast current-driven synthesis (FCDS) method and fabricated ZIF-8 membranes on anodic alumina oxide (AAO) [81]. In the FCDS method, it was found that the formation of ZIF-8 was promoted by the DC current, resulting in the formation of lattice-distorted ZIF-8_Cm as a crystalline polymorph (Figure 6). ZIF-8_Cm, which accounts for 60-70% of the membranes formed, shows higher rigidity and better C_3H_6/C_3H_8 separation than the common cubic ZIF-8_I$\bar{4}$3m, resulting in highest C_3H_6/C_3H_8 selectivity among ZIF-8 membrane reported so far. The methods have been reported to provide sharp molecular sieving ability by suppressing the structural flexibility characteristic of MOFs.

Although the selectivity of ZIF membranes for C_3H_6/C_3H_8 separation has improved significantly, from tens up to about 300, the permeability is still on the order of 10^{-8} mol m^{-2} Pa^{-1} s^{-1} (Table 1). The main reason for this is the membrane thickness, which for most ZIF-8 membranes is several to tens of μm. In contrast, Li et al. developed a gel vapor deposition (GVD) method that combines the sol-gel and chemical vapor deposition methods to fabricate extremely thin ZIF-8 membranes (17~ nm) in PVDF hollow fiber (Figure 7) [82]. The ZIF-8 membranes prepared by the GVD method showed relatively high C_3H_6/C_3H_8 selectivity and one to three orders of magnitude higher permeability than conventional membranes. Ma et al. developed an all-gas phase process for ZIF-8 membrane production [83]. In this method, an ultrathin ZnO layer is deposited on a support by atomic layer deposition (ALD), and then the ZnO layer is converted to ZIF-8 by 2-methylimidazole vapor treatment. The membrane thickness and microstructure are controlled by the number of ALD cycles.

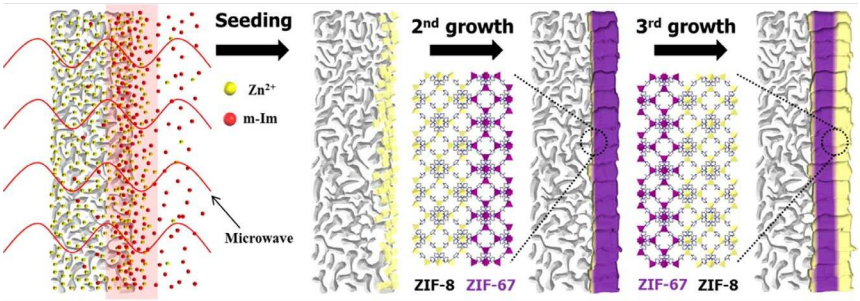

Figure 5. Schematic of ZIF-8/ZIF-67/ZIF-8 membrane synthesis via heteroepitaxial growth. Reprinted with permission from ref. [80]. Copyright 2015 American Chemical Society.

Preprints (www.preprints.org) | NOT PEER-REVIEWED | Posted: 29 December 2023 doi:10.20944/preprints202312.2107.v1

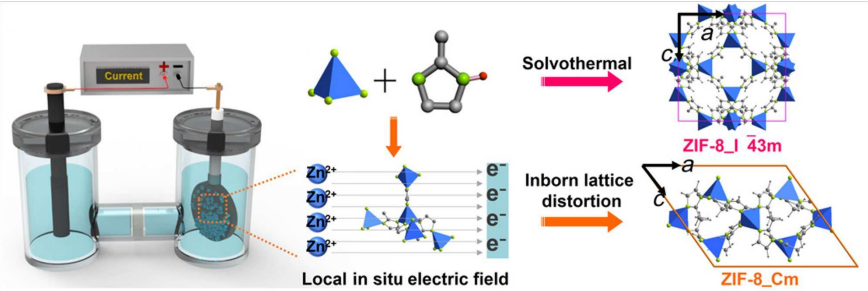

Figure 6. Schematic of the electrochemical cell for ZIF-8 membrane growth by FCDS. The solvothermal route assembles normal I$\bar{4}$3m phase. The inborn lattice distortion occurs and the stiff polymorph ZIF-8_Cm is formed via FCDS. Reproduce from ref. [81] with permission. Copyright 2018 American Association for the Advancement of Science.

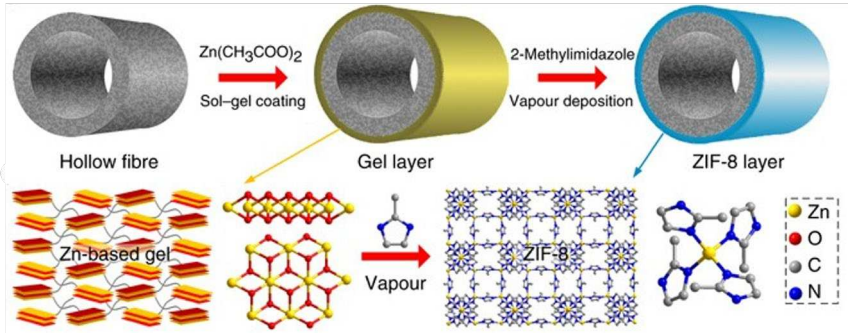

Figure 7. Schematic of the GVD fabrication of ultrathin ZIF-8 membrane. Reprinted with permission from ref. [82]. Copyright 2017 Springer Nature.

5.4. Other Hydrocarbons Separation

Eum et al. applied the IMMP method, which produced ZIF-8 membranes on polyamide-imide hollow fibers, to carbon hollow fibers to produce ZIF-90 membranes [84]. In general, polymer supports have poor chemical resistance and swell when exposed to organic compounds. In contrast, ZIF-90 membranes fabricated on chemically inert carbon hollow fibers exhibited high chemical resistance. ZIF-90, which is composed of Zn(II) and 2-imidazolecarboxaldehyde, has the same crystal topology as ZIF-8 and its crystallographic pore size (3.5 Å) is not much different from that of ZIF-8. On the other hand, its effective pore size (5.0 Å) is larger than ZIF-8 due to its structural flexibility. The ZIF-90 membrane showed *n*-C_4H_{10}/*i*-C_4H_{10} selectivity of 12 and *n*-C_4H_{10} permeability of 6.0×10^{-8} mol m^{-2} Pa^{-1} s^{-1}, indicating its potential for separation of butane isomers.

Huang et al. prepared MIL-160 membranes on porous alumina discs modified with polydopamine and applied them to the separation of xylene isomers [85]. The MIL-160 membranes showed *p*-xylene/*o*-xylene selectivity of 38.5 and *p*-xylene permeation flux of 467 g m^{-2} h^{-1}. MIL-160, which is composed of [$AlO_4(OH)_2$] and 2,5-furan-dicarboxylate as building blocks, has an effective pore size of 5 to 6 Å and shows higher adsorption enthalpy and diffusivity for *p*-xylene than for *o*-xylene. Therefore, MIL-160 membranes are effective for xylene isomer separation and are promising candidates for thermal and chemical stability. In addition, high thermal and chemical stability of MIL-160 membranes is effective for separation of xylene isomers.

5.5. CO_2 Separation

MOF-based membrane research targeting CO_2 separation has been actively investigated [86]. HKUST-1, MIL-53, MIL-100, and MIL-101 are candidates for combustion flue gas, natural gas purification, and hydrogen purification due to their higher CO_2 adsorption capacity than typical zeolites (Table 2) [23,87–98].

Preprints (www.preprints.org) | NOT PEER-REVIEWED | Posted: 29 December 2023 doi:10.20944/preprints202312.2107.v1

Table 2. CO_2 adsorption capacity of typical zeolites and MOFs.

Material		Conditions	CO_2 Adsorption (mmol/g)	Ref.
zeolite	13X	298 K, 21 bar	5.2	[87]
	5A	303 K, 10 bar	3.55	[88]
	DDR	198 K, 1.85 bar	2.8	[89]
	H-ZSM-5	281 K, 0.81 bar	2.15	[90]
	SAPO-34	293 K, 1 bar	3	[91]
MOF	CALF-20	293 K, 1.2 bar	4.07	[92]
	HKUST-1	298 K, 35 bar	10.7	[93]
	MIL-53	304 K, 25 bar	10	[94]
	MIL-100	304 K, 50 bar	18	[23]
	MIL-101	304 K, 50 bar	40	[23]
	MOF-5	298 K, 35 bar	21.7	[93]
	Ni-MOF-74	298 K, 1 bar	6.68	[95]
	Mg-MOF-74	303 K, 1 bar	8.04	[96]
	SIFSIX-3-Cu	298 K, 0.15 bar	2.46	[97]
	ZIF-8	293 K, 1 bar	2.6	[98]

Since H_2/CO_2 is the main separation target for pre-combustion and the molecular size of H_2 is smaller than that of CO_2, research has focused on H_2 selective permeation membranes. Table 3 shows the top data for H_2/CO_2 separation using MOF polycrystalline membranes. MOFs with suitable pore size and high CO_2 affinity can be candidates for CO_2/N_2 separation. CAU-1 with amino groups is one of them (Table 4). The structure of CAU-1 consists of distorted octahedral and tetrahedral cages, which are connected by a triangular window with an opening diameter of 3-4 Å. The amino groups in the CAU-1 framework interacts with CO_2 through acid-base interactions, resulting in improved CO_2/N_2 separation performance. Efficient CO_2/CH_4 separation is very important in natural gas and biogas refining. Corrosion control is important in pipeline transportation, and CO_2 is corrosive in the presence of water vapor, thus it must be kept at low concentrations. Currently, membrane separation accounts for only 10% of the natural gas refining market. If membranes with high permeability and selectivity can be developed, membrane separation may be superior to chemical absorption in natural gas and biogas purification; polycrystalline membranes such as ZIF-8, IRMOF-1, MIL-53-NH_2, and UiO-66 have been reported for CO_2/CH_4 separation applications (Table 5). However, it has been noted that many MOF polycrystalline membranes have low CO_2/CH_4 ideal separation factors. ZIF-8 and MIL-96 have been considered suitable for CO_2/CH_4 separation because their pore entrance diameters are between the molecular sizes of CO_2 and CH_4. However, it should be noted that some MOFs have flexible structures and exhibit dynamic pore characteristics. For example, the effective pore size of ZIF-8 is 4.0-4.2 Å, which is larger than the molecular sizes of CO_2, N_2, and CH_4, and thus does not allow for sharp molecular sieving for CO_2/N_2 and CO_2/CH_4. Ligands with polarizable functional groups and metal nodes with high valence, such as Zr^{4+}, Al^{3+}, Cr^{3+}, and Fe^{3+}, show high adsorption to gas molecules with large quadrupole moments, such as CO_2. On the other hand, strong adsorption may result in low diffusion coefficients. So far, the separation performance of MOF polycrystalline membranes often falls within the trade-off range of higher permeability, but lower selectivity compared to zeolite membranes.

Table 3. H_2/CO_2 separation performance of MOF polycrystalline membranes. (*single gas permeation test).

MOF	Remark	Pore Size (Å)	Method	Support	Q_{H2} (GPU)	$\alpha_{H2/CO2}$	Ref.
CAU-1	$Al_4(OH)_2(OCH_3)_4(NH_2\text{-}bdc)_3$	3.0~4.0	secondary growth	Al_2O_3	322	12.34	[99]
$Co_2(bim)_4$	nanosheet	3.4	vapor phase	GO on Al_2O_3	564	42.7	[100]
HKUST-1	$Cu_3(btc)_2$ (Cu-BTC)	9.0	in situ	PAN	210447	7.14	[65]
HKUST-1			in situ	PMMA	3373	9.24	[101]

Preprints (www.preprints.org) | NOT PEER-REVIEWED | Posted: 29 December 2023 doi:10.20944/preprints202312.2107.v1

JUC-150	$Ni_2(L\text{-}asp)_2(pz)$	3.8×4.7, 2.5×4.5	secondary growth	Ni mesh	546	38.7	[102]
MAMS-1	$Ni_8(5\text{-}bbdc)_6(\mu\text{-}OH)_4$, nanosheet	—	drop cast	AAO	553	235	[103]
NH_2-MIL-53	ammoniated support	8.0	in situ	PVDF	12576	32.35	[104]
NH_2-MIL-53	$Al(OH)(NH_2\text{-}bdc)$	8.0	secondary growth	glass flit	5925	30.9	[105]
Mg-MOF-74	amine-modified	11	in situ	MgO on Al_2O_3	227	28	[106]
SIXSIX-3-Cu	$Cu(bipy)_2(SiF_6)$	3.54	in situ	glass flit	806	8.0	[107]
UiO-67	azobenzene-loaded, light-responsive	10	in situ	Al_2O_3	1316	14.7	[108]
ZIF-7	$Zn(bim)_2$	3.0	in situ	ZnO on PVDF	7027*	18.43*	[109]
ZIF-7	ammoniated support		in situ	Al_2O_3	3051	15.52	[66]
ZIF-8	APTES-modified Al_2O_3	3.4	in situ	Al_2O_3	171044*	17.0*	[110]
ZIF-8	PDA-modified support		in situ	Al_2O_3	71044	8.1	[111]
ZIF-9	$Co(bim)_2$	4.3	in situ	Al_2O_3	22179	14.74*	[112]
ZIF-90	APTES-modified support, post synthetic modification	3.5	in situ	Al_2O_3	884	21.6	[113]
ZIF-95	$Zn(cbim)_2$	3.7	in situ	Al_2O_3	5820	25.7	[114]
$Zn_2(bim)_3$	nanosheet	2.9	drop cast	Al_2O_3	1943	128.4	[115]

Table 4. CO_2/N_2 separation performance of MOF polycrystalline membranes. (*single gas permeation test).

MOF	Remark	Pore Size (Å)	Method	Support	Q_{CO_2} (GPU)	A_{CO_2/N_2}	Ref.
CAU-1	$Al_4(OH)_2(OCH_3)_4(NH_2\text{-}bdc)_3$	3.0~4.0	secondary growth	alumina	3880	22.82	[116]
HKUST-1	$Cu_3(btc)_2$ (Cu-BTC)	9.0	counter-diffusion	alumina	7.3*	33.3*	[117]
IRMOF-1	isoreticular MOF-1 (MOF-5)	11.2	secondary growth	Al_2O_3	615	410	[118]
MIL-100(In)	$In_3O(H_2O)_2OH(btc)_2$	4.6, 8.2	in situ	alumina	5283	3.61*	[119]
SIFSIX-3-Cu	$Cu(bipy)_2(SiF_6)$	3.54	in situ	glass flit	115	0.88	[107]
UiO-66	PDA-modification	6.0	secondary growth	AAO	1116	51.6	[120]
ZIF-8	enzyme-embedded		in situ	PAN	24.16*	165.5*	[121]
ZIF-8	PPSU = polyphenylsulfone, PDMS coating	3.4	LBL	PPSU	925.4*	15.8*	[122]
ZnTCPP	nanosheet	—	filtration, spincoat	PAN	2070*	33*	[123]

Table 5. CO_2/CH_4 separation performance of MOF polycrystalline membranes. (*single gas permeation test).

MOF	Remark	Pore Size (Å)	Method	Support	Q_{CO_2} (GPU)	α_{CO_2/CH_4}	Ref.
CAU-1	$Al_4(OH)_2(OCH_3)_4(NH_2\text{-}bdc)_3$	3.0~4.0	secondary growth	alumina	3940*	14.8*	[116]
HKUST-1	$Cu_3(btc)_2$ (Cu-BTC)	9.0	counter-diffusion	alumina	7.3*	41.5*	[117]
IRMOF-1	isoreticular MOF-1 (MOF-5)	11.2	secondary growth	Al_2O_3	761	328	[118]
NH_2-MIL-53	MOF/organosilica composite	8.0	hot-dipcoat	ceramic fiber	430	18.2	[124]
MIL-96	reactive seeding	3.6×4.5	in situ	Al_2O_3	630*	0.6*	[125]
UiO-66	PDA-modification	6.0	secondary growth	AAO	1179	28.9	[120]
ZIF-8	zeolite/ZIF-8 hybrid		secondary growth	alumina	163	182	[126]
ZIF-8	PPSU = polyphenylsulfone, PDMS coating	3.4	LBL	PPSU	925.4*	17.3*	[122]
ZIF-8	$Zn(OH)_2$ nanostrand precursor		crystal conversion	AAO	3931	2.7	[127]
ZIF-8	ZnAl-NO_3 LDH precursor		crystal conversion	alumina	5.7	16.7	[128]

Preprints (www.preprints.org) | NOT PEER-REVIEWED | Posted: 29 December 2023 doi:10.20944/preprints202312.2107.v1

ZIF-62	$Zn(Im)_{1.75}(Bim)_{0.25}$, MOF glass membrane	1.4	melt-quenching	alumina	36	36.6	[129]
ZIF-94	SIM-1, carboxaldehyde group	2.6	microfluidic	P84®	3.5	37.7	[130]

On the other hand, separation membranes that exceed the upper limit of polymer membrane performance have been reported by using MOF as a filler in a mixed matrix membrane. The combination of polymer matrix and filler is very important. Note that the introduction of fillers can alter the arrangement and free volume of the polymer chains and cause interfacial defects between filler/filler and filler/matrix (Figure 8). Since the affinity between the filler and the polymer matrix plays an important role in the processability and performance of the membrane, the compatibility of both components must also be considered. It has been reported that dispersing MOF fillers in the polymer matrix without interfacial defects improves the separation performance of MMMs due to the molecular sieving effect derived from the uniform pores of the filler (Table 6) [44–61]. Recently, it has also been reported that the synergistic effects of different fillers can be obtained by adding MOF fillers together with graphene oxide (GO) [51] and ionic liquids (ILs) [52] to polymer matrices [53].

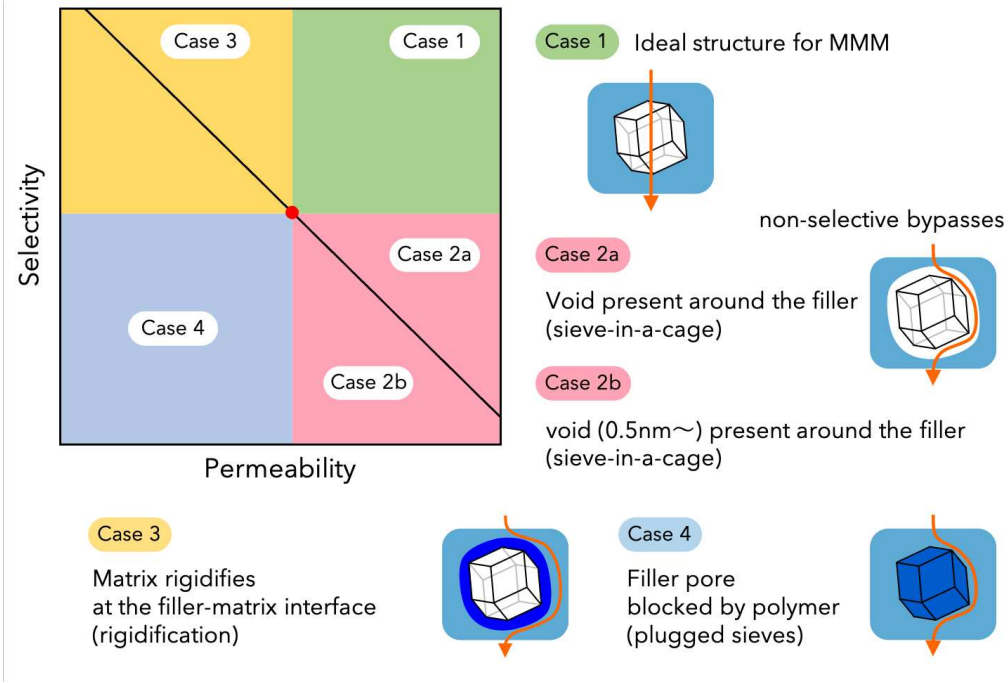

Figure 8. Relationship between filler/matrix interface structure and MMM separation performance.

Table 6. CO_2 separation performance of typical MOF-based MMMs.

Polymer	MOF Filler	Loading	Pressure, Temp.	Permeability (Barrer)	$\alpha_{CO2/N2}$	$\alpha_{CO2/CH4}$	ref.
CA	NH_2-MIL-53(Al)	15 wt%	3 bar, 298 K	—	12	16	[131]
Pebax-1657	NH_2-MIL-53(Al)	10 wt%	10 bar, 308 K	149	55.5	20.5	[132]
PIM-1/Matrimid	NH_2-MIL-53(Al)	25 wt%	2 bar, 298 K	4390	25.0		[133]
6FDA-BI	ZIF-8	20 wt%	4 bar, 298 K	20.3	25.9	57.9	[134]
Pebax-1657	ZIF-8	2 wt%	11 bar, 308 K	118	59	21.4	[135]
PI	ZIF-8	30 wt%	308 K	1437	12	16	[136]
Pebax-2533	ZIF-8	35 wt%	2 bar, RT	1287	32.3	9	[137]
Pebax-2533	ZIF-8 + GO	6 wt%	1 bar, 298 K	220	41	—	[138]
Pebax-1657	ZIF-8 + IL	15 wt%	1 bar, 298 K	104.9	83.9	34.8	[139]
PSF	ZIF-8 + MIL-101(Cr)	16 wt%	2 bar, 308 K	14	40	—	[140]
SPEEK	PEI + MIL-101(Cr)	40 wt%	1 bar, 298 K	2490	80	71.8	[141]

 doi:10.20944/preprints202312.2107.v1

Pebax-1657	ZIF-67	4 wt%	11 bar, 308 K	16	72.7	27.6	[135]
6FDA-Durene	ZIF-71	20 wt%	3.5 bar, 308 K	2560	13.8	14.2	[142]
PIM-1	ZIF-71	30 wt%	3.5 bar, 308 K	8377.1	18.3	11.2	[143]
PIM-1/Matrimid	ZIF-94	25 wt%	2 bar, 298 K	3730	27.1	—	[133]
PIM-1	UiO-66	5 wt%	4 bar, 298 K	2952	26.9	27.3	[144]
PIM-1	UiO-66-CN	20 wt%	1 bar, 298 K	12063.3	53.5	—	[145]
Matrimid®	UiO-66-NH_2	23 wt%	1.4 bar, RT	23.5	36.5	—	[146]
PEO	UiO-66-MA	2 wt%	3.5 bar, 308 K	1450	45.8	—	[147]
PIM-1	MOF-74	20 wt%	2 bar, 298 K	21269	28.7	19.1	[148]

BI: 2-(4-Aminophenyl)-1H-benzimidazol-5-amine, CA: cellulose acetate, Durene: 2,3,5,6-tetramethyl-1,4-phenylenediamine, 6FDA: 4,4-hexafluoroisopropylidene diphtalic anhydride, GO: graphene oxide, NH_2-MIL-53(Al): amino-functionalized MIL-53(Al), IL: ionic liquid, Pebax: poly (ether-block-amide), PEI: polyethylenimine, PEO: polyethylene oxide, PI: polyimide, PSF: polysulfone, SPEEK: sulfonated poly(ether ether ketone), UiO-66-CN: cyano-functionalized UiO-66, UiO-66-MA: isopropenyl-functionalized UiO-66, UiO-66-NH_2: amino-functionalized UiO-66.

6. Conclusions

The development of membrane separation using MOFs has been active due to the rapid increase in the number of studies on MOFs, from synthesis and structural design to application. Relatively long-term durability tests have also been conducted at the laboratory level. Although various MOF-based membranes have been fabricated, the common issue is how to achieve thin membrane formation without generating defects such as pinholes, cracks, and grain boundaries. To this end, it is important to understand the formation mechanism of MOFs based on complexation reactions between metal ions and ligands, and to develop the elementary processes of membrane formation, which can control nucleation and crystal growth. Such fundamental understanding will be the driving force for the next step toward the practical application of separation membranes based on MOFs.

Acknowledgments: This study was supported by the Kansai University Fund for Supporting Outlay Research Centers, 2021. M.S. acknowledges Kansai University's "Scholars from Overseas" program. S.T. acknowledges the support of JKA and its promotion funds from KEIRIN RACE (Grant No. 2023M-412) and the FY2023 research grant program of the Carbon Recycling Fund Institute, Japan.

Conflicts of Interest: The authors declare no conflicts of interest.

References

1. Li, J.R.; Kuppler, R.J.; Zhou, H.C. Selective gas adsorption and separation in metal–organic frameworks. *Chem. Soc. Rev.* **2009**, *38*, 1477–1504.
2. Furukawa, H.; Cordova, K.E.; O'Keeffe, M.; Yaghi, O.M. The chemistry and applications of metal-organic frameworks. *Science* **2013**, *341*, 974–986.
3. Rubio-Martinez, M.; Avci-Camur, C.; Thornton, A.W.; Imaz, I.; Maspoch, D.; Hill, M.R. New synthetic routes towards MOF production at scale. *Chem. Soc. Rev.* **2017**, *46*, 3453–3480.
4. Dai, S.; Tissot, A.; Serre, C. *Bull. Chem. Soc. Jpn.* Metal-organic frameworks: From ambient green synthesis to applications. **2021**, *94*, 2623–2636.
5. Zulkifli, Z.I.; Lim, K.L.; Teh, L.P. Metal-organic frameworks (MOFs) and their applications in CO_2 adsorption and conversion. *ChemistrySelect* **2022**, *7*, e202200572.
6. Petit, C. Present and future of MOF research in the field of adsorption and molecular separation. *Curr. Opin. Chem. Eng.* **2018**, *20*, 132–142.
7. Frameworks for commercial success. *Nat. Chem.* **2016**, *8*, 987.
8. Schneemann, A.; Bon, V.; Schwedler, I.; Senkovska, I.; Kaskel, S.; Fischer, R.A. Flexible metal–organic frameworks. *Chem. Soc. Rev.* **2014**, 43, 6062–6096.
9. Sakata, Y.; Furukawa, S.; Kondo, M.; Hirai, K.; Horike, N.; Takashima, Y.; Uehara, H.; Louvain, N.; Meilikhov, M.; Tsuruoka, T.; Isoda, S.; Kosaka, W.; Sakata, O.; Kitagawa, S. Shape-memory nanopores induced in coordination frameworks by crystal downsizing. *Science* **2013**, *339*, 193–196.

10. Tanaka, S.; Fujita, K.; Miyake, Y.; Miyamoto, M.; Hasegawa, Y.; Makino, T.; Van der Perre, S.; Remi, J.C.S.; Van Assche, T.; Baron, G.V.; Denayer, J.F.M. Adsorption and diffusion phenomena in crystal size engineered ZIF-8 MOF. *J. Phys. Chem. C* **2015**, *119*, 28430–28439.
11. Devic, T.; Serre, C. High valence 3p and transition metal based MOFs. *Chem. Soc. Rev.* **2014**, *43*, 6097–6115.
12. Park, K.S.; Ni, Z.; Côté, A.P.; Choi, J.Y.; Huang, R.; Uribe-Romo, F.J.; Chae, H.K.; O'Keeffe, M.; Yaghi, O.M. Exceptional chemical and thermal stability of zeolitic imidazolate frameworks. *Proc. Natl. Acad. Sci. USA* **2006**, *103*, 10186–10191.
13. Wang, Q.M.; Shen, D.M.; Bulow, M.; Lau, M.L.; Deng, S.G.; Fitch, F.R.; Lemcoff, N.O.; Semanscin, J. Metallo-organic molecular sieve for gas separation and purification. *Microporous Mesoporous Mater.* **2002**, *55*, 217–230.
14. Lin, K.S.; Adhikari, A.K.; Ku, C.N.; Chiang, C.L.; Kuo, H. Synthesis and characterization of porous HKUST-1 metal organic frameworks for hydrogen storage. *Int. J. Hydrogen Energy* **2012**, *37*, 13865–13871.
15. Lamia, N.; Jorge, M.; Granato, M.A.; Almeida, P.F.A.; Chevreau, H.; Rodrigues, A.E. Adsorption of propane, propylene and isobutane on a metal–organic framework: Molecular simulation and experiment. *Chem. Eng. Sci.* **2009**, *64*, 3246–3259.
16. Abednatanzi, S.; Gohari, D.P.; Depauw, H.; Coudert, F.X.; Vrielinck, H.; Van Der Voort, P.; Leus, K. Mixed-metal metal–organic frameworks. *Chem. Soc. Rev.* **2019**, *48*, 2535–2565.
17. Hong, D.Y.; Hwang, Y.K.; Serre, C.; Férey, G.; Chang, J.S. Porous chromium terephthalate MIL-101 with coordinatively unsaturated sites: Surface functionalization, encapsulation, sorption and catalysis. *Adv. Funct. Mater.* **2009**, *19*, 1537–1552.
18. Jiang, D.; Keenan, L.L.; Burrows, A.D.; Edler, K.J. Synthesis and post-synthetic modification of MIL-101(Cr)-NH_2 via a tandem diazotisation process. *Chem. Commun.* **2012**, *48*, 12053–12055.
19. Ren, J.; Musyoka, N.M.; Langmi, H.W.; Segakweng, T.; North, B.C.; Mathe, M.; Kang, X. Modulated synthesis of chromium-based metal-organic framework (MIL-101) with enhanced hydrogen uptake. *Int. J. Hydrogen Energy* **2014**, *39*, 12018–12023.
20. Yuan, S.; Feng, L.; Wang, K.; Pang, J.; Bosch, M.; Lollar, C.; Sun, Y.; Qin, J.; Yang, X.; Zhang, P. Stable metal–organic frameworks: Design, synthesis, and applications. *Adv. Mater.* **2018**, *30*, 1704303.
21. Latroche, M.; Surblé, S.; Serre, C.; Mellot-Draznieks, C.; Llewellyn, P.L.; Lee, J.H.; Chang, J.S.; Jhung, S.H.; Férey, G. Hydrogen storage in the giant-pore metal–organic frameworks MIL-100 and MIL-101. *Angew. Chem., Int. Ed.* **2006**, *45*, 8227–8231.
22. Horcajada, P.; Surblé, S.; Serre, C.; Hong, D.Y.; Seo, Y.K.; Chang, J.S.; Grenèche, J.M.; Margiolaki, I.; Férey, G. Synthesis and catalytic properties of MIL-100(Fe), an iron(iii) carboxylate with large pores. *Chem. Commun.* **2007**, 2820–2822.
23. Llewellyn, P.L.; Bourrelly, S.; Serre, C.; Vimont, A.; Daturi, M.; Hamon, L.; De Weireld, G.; Chang, J.S.; Hong, D.Y.; Hwang, Y.K. High uptakes of CO_2 and CH_4 in mesoporous metal—Organic frameworks MIL-100 and MIL-101. *Langmuir* **2008**, *24*, 7245–7250.
24. Yoon, J.W.; Seo, Y.K.; Hwang, Y.K.; Chang, J.S.; Leclerc, H.; Wuttke, S.; Bazin, P.; Vimont, A.; Daturi, M.; Bloch, E. Controlled reducibility of a metal–organic framework with coordinatively unsaturated sites for preferential gas sorption. *Angew. Chem., Int. Ed.* **2010**, *49*, 5949–5952.
25. Lee, S.J.; Yoon, J.W.; Seo, Y.K.; Kim, M.B.; Lee, S.K.; Lee, U.H.; Hwang, Y.K.; Bae, Y.S.; Chang, J.S. Effect of purification conditions on gas storage and separations in a chromium-based metal-organic framework MIL-101. *Microporous Mesoporous Mater.* **2014**, *193*, 160–165.
26. Chang, G.; Bao, Z.; Ren, Q.; Deng, S.; Zhang, Z.; Su, B.; Xing, H.; Yang, Y. Fabrication of cuprous nanoparticles in MIL-101: An efficient adsorbent for the separation of olefin–paraffin mixtures. *RSC Adv.* **2014**, *4*, 20230–20233.
27. Zhang, Y.; Li, B.; Krishna, R.; Wu, Z.; Ma, D.; Shi, Z.; Pham, T.; Forrest, K.; Space, B.; Ma, S.; Highly selective adsorption of ethylene over ethane in a MOF featuring the combination of open metal site and π-complexation. *Chem. Commun.* **2015**, *51*, 2714–2717.
28. Kim, A.R.; Yoon, T.U.; Kim, E.J.; Yoon, J.W.; Kim, S.Y.; Yoon, J.W.; Hwang, Y.K.; Chang, J.S.; Bae, Y.S. Facile loading of Cu (I) in MIL-100 (Fe) through redox-active Fe (II) sites and remarkable propylene/propane separation performance. *Chem. Eng. J.* **2018**, *331*, 777–784.
29. Bao, Z.; Alnemrat, S.; Yu, L.; Vasiliev, I.; Ren, Q.; Lu, X.; Deng, S. Adsorption of ethane, ethylene, propane, and propylene on a magnesium-based metal–organic framework. *Langmuir* **2011**, *27*, 13554–13562.
30. Bae, Y.S.; Lee, C.Y.; Kim, K.C.; Farha, O.K.; Nickias, P.; Hupp, J.T.; Nguyen, S.T.; Snurr, R.Q. High propene/propane selectivity in isostructural metal–organic frameworks with high densities of open metal sites. *Angew. Chem., Int. Ed.* **2012**, *51*, 1857–1860.
31. Bachman, J.E.; Kapelewski, M.T.; Reed, D.A.; Gonzalez, M.I.; Long, J.R. M_2(m-dobdc) (M = Mn, Fe, Co, Ni) metal–organic frameworks as highly selective, high-capacity adsorbents for olefin/paraffin separations. *J. Am. Chem. Soc. 2017*, **139**, 15363–15370.

32. Yang, S.; Ramirez-Cuesta, A.J.; Newby, R.; Garcia-Sakai, V.; Manuel, P.; Callear, S.K.; Campbell, S.I.; Tang, C.C.; Schroder, M. Supramolecular binding and separation of hydrocarbons within a functionalized porous metal–organic framework. *Nat. Chem.* **2014**, *7*, 121–129.
33. Gücüyener, C.; van den Bergh, J.; Gascon, J.; Kapteijn, F. Ethane/ethene separation turned on its head: Selective ethane adsorption on the metal−organic framework ZIF-7 through a gate-opening mechanism. *J. Am. Chem. Soc.* **2010**, *132*, 17704–17706.
34. van den Bergh, J.; Gucuyener, C.; Pidko, E.A.; Hensen, E.J.M.; Gascon, J.; Kapteijn, F. *Chem. -Eur. J.* **2011**, *17*, 8832–8840.
35. Liao, P.Q.; Zhang, W.X.; Zhang, J.P.; Chen, X.M. Efficient purification of ethene by an ethane-trapping metal-organic framework. *Nat. Commun.* **2015**, *6*, 8697.
36. Kishida, K.; Okumura, Y.; Watanabe, Y.; Mukoyoshi, M.; Bracco, S.; Comotti, A.; Sozzani, P.; Horike, S.; Kitagawa, S. Recognition of 1,3-butadiene by a porous coordination polymer. *Angew. Chem., Int. Ed.* **2016**, *55*, 13784–13788.
37. Zhu, W.; Kapteijn, F.; Moulijn, J.A.; Jansen, J.C. Selective adsorption of unsaturated linear C_4 molecules on the all-silica DD3R. *Phys. Chem. Chem. Phys.* **2000**, *2*, 1773–1779.
38. Hartmann, M.; Kunz, S.; Himsl, D.; Tangermann, O.; Ernst, S.; Wagener, A. Adsorptive separation of isobutene and isobutane on $Cu_3(BTC)_2$. *Langmuir* **2008**, *24*, 8634–8642.
39. Lange, M.; Kobalz, M.; Bergmann, J.; Lässig, D.; Lincke, J.; Möllmer, J.; Möller, A.; Hofmann, J.; Krautscheid, H.; Staudt, R.; Gläser, R. Structural flexibility of a copper-based metal–organic framework: Sorption of C_4-hydrocarbons and in situ XRD. *J. Mater. Chem. A* **2014**, *2*, 8075–8085.
40. Ye, Z.M.; He, C.T.; Xu, Y.T.; Krishna, R.; Xie, Y.; Zhou, D.D.; Zhou, H.L.; Zhang, J.P.; Chen, X.M. A new isomeric porous coordination framework showing single-crystal to single-crystal structural transformation and preferential adsorption of 1,3-butadiene from C4 hydrocarbons. *Cryst. Growth Des.* **2017**, *17*, 2166–2171.
41. Pan, L.; Olson, D.H.; Ciemnolonski, L.R.; Heddy, R.; Li, J. Separation of hydrocarbons with a microporous metal–organic framework. *Angew. Chem., Int. Ed.* **2006**, *45*, 616–619.
42. Peralta, D.; Chaplais, G.; Simon-Masseron, A.; Barthelet, K.; Pirngruber, G.D. Separation of C_6 paraffins using zeolitic imidazolate frameworks: Comparison with zeolite 5A. *Ind. Eng. Chem. Res.* **2012**, *51*, 4692–4702.
43. Alaerts, L.; Kirschhock, C.E.; Maes, M.; van der Veen, M.A.; Finsy, V.; Depla, A.; Martens, J.A.; Baron, G.V.; Jacobs, P.A.; Denayer, J.F.M.; De Vos, D.E. Selective Adsorption and separation of xylene isomers and ethylbenzene with the microporous vanadium(IV) terephthalate MIL-47. *Angew. Chem., Int. Ed.* **2007**, *46*, 4293–4297.
44. Alaerts, L.; Maes, M.; Jacobs, P.A.; Denayer, J.F.M.; De Vos, D.E. Activation of the metal-organic framework MIL-47 for selective adsorption of xylenes and other difunctionalized aromatics. *Phys. Chem. Chem. Phys.* **2008**, *10*, 2979–2985.
45. Alaerts, L.; Maes, M.; Giebeler, L.; Jacobs, P.A.; Martens, J.A.; Denayer, J.F.M.; Kirschhock, C.E.A.; De Vos, D.E. Selective adsorption and separation of ortho-substituted alkylaromatics with the microporous aluminum terephthalate MIL-53. *J. Am. Chem. Soc.* **2008**, *130*, 14170–14178.
46. Finsy, V.; Verelst, H.; Alaerts, L.; De Vos, D.; Jacobs, P.A.; Baron, G.V.; Denayer, J.F.M. Pore-filling-dependent selectivity effects in the vapor-phase separation of xylene isomers on the metal−organic framework MIL-47. *J. Am. Chem. Soc.* **2008**, *130*, 7110–7118.
47. Finsy, V.; Christine, E.A.; Kirschhock, C.E.; Vedts, G.; Maes, M.; Alaerts, L.; De Vos, D.E.; Baron, G.V.; Denayer, J.F.M. Framework breathing in the vapour-phase adsorption and separation of xylene isomers with the metal–organic framework MIL-53. *Chem. Eur. J.* **2009**, *15*, 7724–7731.
48. Bárcia, P.S.; Guimarães, D.; Mendes, P.A.P.; Silva, J.A.C.; Guillerm, V.; Chevreau, H.; Serre, C.; Rodrigues, A.E. Reverse shape selectivity in the adsorption of hexane and xylene isomers in MOF UiO-66. *Microporous Mesoporous Mater.* **2011**, *139*, 67–73.
49. Schlissel, D.W.D.; Wamsted, D. Holy Grail of Carbon Capture Continues to Elude Coal Industry. *Institute for Energy Economics and Financial Analysis* **2018**.
50. Refinitiv carbon market survey 2021. https://www.refinitiv.com/ (accessed on 24th June 2021).
51. Kamio, E.; Yoshioka, T. Membrane separation technology for CO_2 separation and recovery in Japan. *Membrane* **2017**, *42*, 2–10.
52. Hermes, S.; Schroder, F.; Chelmowski, R.; Wöll, C.; Fischer, R. A. Selective nucleation and growth of metal−organic open framework thin films on patterned COOH/CF_3-terminated self-assembled monolayers on Au(111). *J. Am. Chem. Soc.* **2005**, *127*, 13744–13745.
53. Arnold, M.; Kortunov, P.; Jones, D.J.; Nedellec, Y.; Kärger, J.; Caro, J. Oriented crystallisation on supports and anisotropic mass transport of the metal-organic framework manganese formate. *Eur. J. Inorg. Chem.* **2007**, 60–64.
54. Scherb, C.; Schodel, A.; Bein, T. Directing the structure of metal–organic frameworks by oriented surface growth on an organic monolayer. *Angew. Chem. Int. Ed.* **2008**, *47*, 5777–5779.

55. Gascon, J.; Aguado, S.; Kapteijn, F. Manufacture of dense coatings of $Cu_3(BTC)_2$ (HKUST-1) on α-alumina. *Micropor. Mesopor. Mater.* **2008**, *113*, 132–138.
56. Lin, R.J.; Hernandez, B.V.; Ge, L.; Zhu, Z.H. Metal organic framework based mixed matrix membranes: An overview on filler/polymer interfaces. *J. Mater. Chem. A* **2018**, *6*, 293–312.
57. Liu, Y.; Zeng, G.; Pan, Y.; Lai, Z. Synthesis of highly *c*-oriented ZIF-69 membranes by secondary growth and their gas permeation properties. *J. Membr. Sci.* **2011**, *379*, 46–51.
58. Zheng, B.; Pan, Y.; Lai, Z.; Huang, K.W. Molecular dynamics simulations on gate opening in ZIF-8: Identification of factors for ethane and propane separation. *Langmuir* **2013**, *29*, 8865–8872.
59. Venna, S.R.; Carreon, M.A. Highly permeable zeolite imidazolate framework-8 membranes for CO_2/CH_4 separation. *J. Am. Chem. Soc.* **2010**, *132*, 76–78.
60. Lee, J.H.; Kim, D.; Shin, H.; Yoo, S.J.; Kwon, H.T.; Kim, J. Zeolitic imidazolate framework ZIF-8 films by ZnO to ZIF-8 conversion and their usage as seed layers for propylene-selective ZIF-8 membranes. *J. Ind. Eng. Chem.* **2019**, *72*, 374–379.
61. Huang, A.; Bux, H.; Steinbach, F.; Caro, J. Molecular-sieve membrane with hydrogen permselectivity: ZIF-22 in LTA topology prepared with 3-aminopropyltriethoxysilane as covalent linker. *Angew. Chem., Int. Ed.* **2010**, *49*, 4958–4961.
62. McCarthy, M.C.; Guerrero, V.V.; Barnett, G.V.; Jeong, H.K. Synthesis of zeolitic imidazolate framework films and membranes with controlled microstructures. *Langmuir* **2010**, *26*, 14636–14641.
63. Tanaka, S.; Shimada, T.; Fujita, K.; Miyake, Y.; Kida, K.; Yogo, K.; Denayer, J.F.M.; Sugita, M.; Takewaki, T. Seeding-free aqueous synthesis of zeolitic imidazolate framework-8 membranes: How to trigger preferential heterogeneous nucleation and membrane growth in aqueous rapid reaction solution. *J. Membr. Sci.* **2014**, *472*, 29–38.
64. Tanaka, S.; Okubo, K.; Kida, K.; Sugita, M.; Takewaki, T. Grain size control of ZIF-8 membranes by seeding-free aqueous synthesis and their performances in propylene/propane separation. *J. Membr. Sci.* **2017**, *544*, 306–311.
65. Li, W.; Yang, Z.; Zhang, G.; Fan, Z.; Meng, Q.; Shen, C.; Gao, C. Stiff metal–organic framework–polyacrylonitrile hollow fiber composite membranes with high gas permeability. *J. Mater. Chem. A* **2014**, *2*, 2110–2118.
66. Li, W.; Meng, Q.; Zhang, C.; Zhang, G. Metal–organic framework/PVDF composite membranes with high H_2 permselectivity synthesized by ammoniation. *Chem. Eur. J.* **2015**, *21*, 7224–7230.
67. Yao, J.; Dong, D.; Li, D.; He, L.; Xu, G.; Wang, H. Contra-diffusion synthesis of ZIF-8 films on a polymer substrate. *Chem. Commun.* **2011**, *47*, 2559–2561.
68. Know, H.T.; Jeong, H.K. In situ synthesis of thin zeolitic–imidazolate framework ZIF-8 membranes exhibiting exceptionally high propylene/propane separation. *J. Am. Chem. Soc.* **2013**, *135*, 10763–10768.
69. Hara, N.; Yoshimune, M.; Negishi, H.; Haraya, K.; Hara, S.; Yamaguchi, T. Diffusive separation of propylene/propane with ZIF-8 membranes. *J. Membr. Sci.* **2014**, *450*, 215–223.
70. Dong, X.; Huang, K.; Liu, S.; Ren, R.; Jin, W.; Lin, Y.S. Synthesis of zeolitic imidazolate framework-78 molecular-sieve membrane: Defect formation and elimination. *J. Mater. Chem.* **2012**, *22*, 19222–19227.
71. Guerrero, V.V.; Yoo, Y.; McCarthy, M.C.; Jeong, H.K. HKUST-1membranes on porous supports using secondary growth. *J. Mater. Chem.* **2010**, *20*, 3938–3943.
72. Zhang, K.; Lively, R.P.; Zhang, C.; Chance, R.R.; Koros, W.J.; Sholl, D.S.; Nair, S. Exploring the framework hydrophobicity and flexibility of ZIF-8: From biofuel recovery to hydrocarbon separations. *J. Phys. Chem. Lett.* **2013**, *4*, 3618–3622.
73. Bux, H.; Chmelik, C.; van Baten, J.M.; Krishna, R.; Caro, J. Novel MOF-membrane for molecular sieving predicted by IR-diffusion studies and molecular modeling. *Adv. Mater.* **2010**, *22*, 4741–4743.
74. Li, K.; Olson, D.H.; Seidel, J.; Emge, T.J.; Gong, H.; Zeng, H.; Li, J. Zeolitic imidazolate frameworks for kinetic separation of propane and propene. *J. Am. Chem. Soc.* **2009**, *131*, 10368–10369.
75. Pan, Y.; Lai, Z. Sharp separation of C2/C3 hydrocarbon mixtures by zeolitic imidazolate framework-8 (ZIF-8) membranes synthesized in aqueous solutions. *Chem. Commun.* **2011**, *47*, 10275–10277.
76. Bux, H.; Chmelik, C.; Krishna, R.; Caro, J. Ethene/ethane separation by the MOF membrane ZIF-8: Molecular correlation of permeation, adsorption, diffusion. *J. Membr. Sci.* **2011**, *369*, 284–289.
77. Zhang, C.; Lively, R.P.; Zhang, K.; Johnson, J.R.; Karvan, O.; Koros, W.J. Unexpected molecular sieving properties of zeolitic imidazolate framework-8. *J. Phys. Chem. Lett.* **2012**, *3*, 2130–2134.
78. Brown, A.J.; Brunelli, N.A.; Eum, K.; Rashidi, F.; Johnson, J.R.; Koros, W.J.; Jones, C.W.; Nair, S. Interfacial microfluidic processing of metal-organic framework hollow fiber membranes. *Science* **2014**, *345*, 72–75.
79. Eum, K.; Ma, C.; Rownaghi, A.; Jones, C.W.; Nair, S. ZIF-8 membranes via interfacial microfluidic processing in polymeric hollow fibers: Efficient propylene separation at elevated pressures. *ACS Appl. Mater. Interfaces* **2016**, *8*, 25337–25342.
80. Kwon, H.T.; Jeong, H.K.; Lee, A.S.; An, H.S.; Lee, J.S. Heteroepitaxially grown zeolitic imidazolate framework membranes with unprecedented propylene/propane separation performances. *J. Am. Chem. Soc.* **2015**, *137*, 12304–12311.

81. Zhou, S.; Wei, Y.; Li, L.; Duan, Y.; Hou, Q.; Zhang, L.; Ding, L.X.; Xue, J.; Wang, H.; Caro, J. Paralyzed membrane: Current-driven synthesis of a metal-organic framework with sharpened propene/propane separation. *Science Adv.* **2018**, *4*, eaau1393.
82. Li, W.; Su, P.; Li, Z.; Xu, Z.; Wang, F.; Ou, H.; Zhang, J.; Zhang, G.; Zeng, E. Ultrathin metal–organic framework membrane production by gel–vapour deposition. *Nat. Commun.* **2017**, *8*, 406.
83. Ma, X.; Kumar, P.; Mittal, N.; Khlyustova, A.; Daoutidis, P.; Mkhoyan, K.A.; Tsapatsis, M. Zeolitic imidazolate framework membranes made by ligand-induced permselectivation. *Science* **2018**, *361*, 1008–1011.
84. Eum, K.; Ma, C.; Koh, D.Y.; Rashidi, F.; Li, Z.; Jones, C.W.; Lively, R.P.; Nair, S. Zeolitic imidazolate framework membranes supported on macroporous carbon hollow fibers by fluidic processing techniques. *Adv. Mater. Interfaces* **2017**, *4*, 1700080.
85. Wu, X.; Wei, W.; Jiang, J.; Caro, J.; Huang, A. High-flux high-selectivity metal–organic framework MIL-160 membrane for xylene isomer separation by pervaporation. *Angew. Chem., Int. Ed.* **2018**, *57*, 15354–15358.
86. Venna, S.R.; Carreon, M.A. Metal organic framework membranes for carbon dioxide separation. *Chem. Eng. Sci.* **2015**, *124*, 3–19.
87. Dunne, J.; Myers, A.L. Adsorption of gas mixtures in micropores: Effect of difference in size of adsorbate molecules. *Chem. Eng. Sci.* **1994**, *49*, 2941–2951.
88. Pakseresht, S.; Kazemeini, M.; Akbarnejad, M.M. Equilibrium isotherms for CO, CO_2, CH_4 and C_2H_4 on the 5A molecular sieve by a simple volumetric apparatus. *Sep. Purif. Technol.* **2002**, *28*, 53–60.
89. Maghsoudi, H.; Soltanieh, M.; Bozorgzadeh, H.; Mohamadalizadeh, A. Adsorption isotherms and ideal selectivities of hydrogen sulfide and carbon dioxide over methane for the Si-CHA zeolite: Comparison of carbon dioxide and methane adsorption with the all-silica DD3R zeolite. *Adsorption* **2013**, *19*, 1045–1053.
90. Calleja, G.; Pau, J.; Calles, J.A. Pure and multicomponent adsorption equilibrium of carbon dioxide, ethylene, and propane on ZSM-5 zeolites with different Si/Al ratios. *J. Chem. Eng. Data* **1998**, *43*, 994–1003.
91. Venna, S.R.; Carreon, M.A. Synthesis of SAPO-34 crystals in the presence of crystal growth inhibitors. *J. Phys. Chem. B* **2008**, *112*, 16261–16265.
92. Lin, J.B.; Nguyen, T.T.T.; Vaidhyanathan, R.; Burner, J.; Taylor, J.M.; Durekova, H.; Akhtar, F.; Mah, R.K.; Ghaffari-Nik, O.; Marx, S.; Fylstra, N.; Iremonger, S.S.; Dawson, K.W.; Sarkar, P.; Hovington, P.; Rajendran, A.; Woo, T.K.; Shimizu, G.K.H. A scalable metal-organic framework as a durable physisorbent for carbon dioxide capture. *Science* **2021**, *374*, 1464–1469.
93. Millward, A.R.; Yaghi, O.M. Metal–organic frameworks with exceptionally high capacity for storage of carbon dioxide at room temperature. *J. Am. Chem. Soc.* **2005**, *127*, 17998–17999.
94. Bourrelly, S.; Llewellyn, P.L.; Serre, C.; Millange, F.; Loiseau, T.; Férey, G. Different adsorption behaviors of methane and carbon dioxide in the isotypic nanoporous metal terephthalates MIL-53 and MIL-47. *J. Am. Chem. Soc.* **2005**, *127*, 13519–13521.
95. Liu, J.; Wang, Y.; Benin, A.I.; Jakubczak, P.; Willis, R.R.; LeVan, M.D. CO_2/H_2O adsorption equilibrium and rates on metal–organic frameworks: HKUST-1 and Ni/DOBDC. *Langmuir* **2010**, *26*, 14301–14307.
96. Mason, J.A.; Sumida, K.; Herm, Z.R.; Krishna, R.; Long, J.R. Evaluating metal–organic frameworks for post-combustion carbon dioxide capture *via* temperature swing adsorption. *Energy Environ. Sci.* **2011**, *4*, 3030–3040.
97. Shekhah, O.; Belmabkhout, Y.; Chen, Z.; Guillerm, V.; Cairns, A.; Adil, K.; Eddaoudi, M. Made-to-order metal-organic frameworks for trace carbon dioxide removal and air capture. *Nat. Commun.* **2014**, *5*, 4228.
98. Venna, S.R.; Zhu, M.Q.; Li, S.G.; Carreon, M.A. Knudsen diffusion through ZIF-8 membranes synthesized by secondary seeded growth. *J. Porous Mater.* **2014**, *21*, 235–240.
99. Zhou, S.; Zou, X.; Sun, F.; Ren, H.; Liu, J.; Zhang, F.; Zhao, N.; Zhu, G. Development of hydrogen-selective CAU-1 MOF membranes for hydrogen purification by 'dual-metal-source' approach. *Int. J. Hydrogen Energy* **2013**, *38*, 5338–5347.
100. Nian, P.; Liu, H.; Zhang, X. Bottom-up fabrication of two-dimensional Co-based zeolitic imidazolate framework tubular membranes consisting of nanosheets by vapor phase transformation of Co-based gel for H_2/CO_2 separation. *J. Membr. Sci.* **2019**, *573*, 200–209.
101. Ben, T.; Lu, C.; Pei, C.; Xu, S.; Qiu, S. Polymer-supported and free-standing metal–organic framework membrane. *Chem. Eur. J.* **2012**, *18*, 10250–10253.
102. Kang, Z.; Xue, M.; Fan, L.; Huang, L.; Guo, L.; Wei, G.; Chen, B.; Qiu, S. Highly selective sieving of small gas molecules by using an ultra-microporous metal–organic framework membrane. *Energy Environ. Sci.* **2014**, *7*, 4053–4060.
103. Wang, X.; Chi, C.; Zhang, K.; Qian, Y.; Gupta, K.M.; Kang, Z.; Jiang, J.; Zhao, D. Reversed thermo-switchable molecular sieving membranes composed of two-dimensional metal-organic nanosheets for gas separation. *Nat. Commun.* **2017**, *8*, 14460.
104. Li, W.; Su, P.; Zhang, G.; Shen, C.; Meng, Q. Preparation of continuous NH_2–MIL-53 membrane on ammoniated polyvinylidene fluoride hollow fiber for efficient H_2 purification. *J. Membr. Sci.* **2015**, *495*, 384–391.

105. Zhang, F.; Zou, X.; Gao, X.; Fan, S.; Sun, F.; Ren, H.; Zhu, G. Hydrogen selective NH_2-MIL-53(Al) MOF membranes with high permeability. *Adv. Funct. Mater.* **2012**, *22*, 3583–3590.
106. Wang, N.; Mundstock, A.; Liu, Y.; Huang, A.; Caro, J. Amine-modified Mg-MOF-74/CPO-27-Mg membrane with enhanced H_2/CO_2 separation. *Chem. Eng. Sci.* **2015**, *124*, 27–36.
107. Fan, S.; Sun, F.; Xie, J.; Guo, J.; Zhang, L.; Wang, C.; Pan, Q.; Zhu, G.; Facile synthesis of a continuous thin $Cu(bipy)_2(SiF_6)$ membrane with selectivity towards hydrogen. *J. Mater. Chem. A* **2013**, *1*, 11438–11442.
108. Knebel, A.; Sundermann, L.; Mohmeyer, A.; Strauß, I.; Friebe, S.; Behrens, P.; Caro, J. Azobenzene guest molecules as light-switchable CO_2 valves in an ultrathin UiO-67 membrane. *Chem. Mater.* **2017**, *29*, 3111–3117.
109. Li, W.; Meng, Q.; Li, X.; Zhang, C.; Fan, Z.; Zhang, G. Non-activation ZnO array as a buffering layer to fabricate strongly adhesive metal–organic framework/PVDF hollow fiber membranes. *Chem. Commun.* **2014**, *50*, 9711–9713.
110. Xie, Z.; Yang, J.; Wang, J.; Bai, J.; Yin, H.; Yuan, B.; Lu, J.; Zhang, Y.; Zhou, L.; Duan, C. Deposition of chemically modified α-Al_2O_3 particles for high performance ZIF-8 membrane on a macroporous tube. *Chem. Commun.* **2012**, *48*, 5977–5979.
111. Huang, A.; Liu, Q.; Wang, N.; Caro, J. Highly hydrogen permselective ZIF-8 membranes supported on polydopamine functionalized macroporous stainless-steel-nets. *J. Mater. Chem. A* **2014**, *2*, 8246–8251.
112. Huang, Y.; Liu, D.; Liu, Z.; Zhong, C. Synthesis of zeolitic imidazolate framework membrane using temperature-switching synthesis strategy for gas separation. *Ind. Eng. Chem. Res.* **2016**, *55*, 7164–7170.
113. Huang, A.; Wang, N.; Kong, C.; Caro, J. Organosilica-functionalized zeolitic imidazolate framework ZIF-90 membrane with high gas-separation performance. *Angew. Chem., Int. Ed.* **2012**, *51*, 10551–10555.
114. Huang, A.; Chen, Y.; Wang, N.; Hu, Z.; Jiang, J.; Caro, J. A highly permeable and selective zeolitic imidazolate framework ZIF-95 membrane for H_2/CO_2 separation. *Chem. Commun.* **2012**, *48*, 10981–10983.
115. Peng, Y.; Li, Y.; Ban, Y.; Yang, W. Two-dimensional metal–organic framework nanosheets for membrane-based gas separation. *Angew. Chem., Int. Ed.* **2017**, *56*, 9757–9761.
116. Yin, H.; Wang, J.; Xie, Z.; Yang, J.; Bai, J.; Lu, J.; Zhang, Y.; Yin, D.; Lin, J.Y.S. A highly permeable and selective amino-functionalized MOF CAU-1 membrane for CO_2–N_2 separation. *Chem. Commun.* **2014**, *50*, 3699–3701.
117. Hara, N.; Yoshimune, M.; Negishi, H.; Haraya, K.; Hara, S.; Yamaguchi, T. Metal–organic framework membranes with layered structure prepared within the porous support. *RSC Adv.* **2013**, *3*, 14233–14236.
118. Rui, Z.; James, J.B.; Kasik, A.; Lin, Y.S. Metal-organic framework membrane process for high purity CO_2 production. *AIChE J.* **2016**, *62*, 3836–3841.
119. Dou, Z.; Cai, J.; Cui, Y.; Yu, J.; Xia, T.; Yang, Y.; Qian, G. Preparation and gas separation properties of metal-organic framework membranes. *Z. Anorg. Allg. Chem.* **2015**, *641*, 792–796.
120. Wu, W.; Li, Z.; Chen, Y.; Li, W. Polydopamine-modified metal–organic framework membrane with enhanced selectivity for carbon capture. *Environ. Sci. Technol.* **2019**, *53*, 3764–3772.
121. Zhang, Y.; Wang, H.; Liu, J.; Hou, J.; Zhang, Y. Enzyme-embedded metal–organic framework membranes on polymeric substrates for efficient CO_2 capture. *J. Mater. Chem. A* **2017**, *5*, 19954–19962.
122. Jomekian, A.; Behbahani, R.M.; Mohammadi, T.; Kargari, A. Innovative layer by layer and continuous growth methods for synthesis of ZIF-8 membrane on porous polymeric support using poly(ether-*block*-amide) as structure directing agent for gas separation. *Microporous Mesoporous Mater.* **2016**, *234*, 43–54.
123. Liu, M.; Xie, K.; Nothling, M.D.; Gurr, P.A.; Tan, S.S.L.; Fu, Q.; Webley, P.A.; Qiao, G.G. Ultrathin Metal–Organic Framework Nanosheets as a Gutter Layer for Flexible Composite Gas Separation Membranes. *ACS Nano* **2018**, *12*, 11591–11599.
124. Kong, C.; Du, H.; Chen, L.; Chen, B. Nanoscale MOF/organosilica membranes on tubular ceramic substrates for highly selective gas separation. *Energy Environ. Sci.* **2017**, *10*, 1812–1819.
125. Nan, J.; Dong, X.; Wang, W.; Jin, W. Formation mechanism of metal–organic framework membranes derived from reactive seeding approach. *Microporous Mesoporous Mater.* **2012**, *155*, 90–98.
126. Yeo, Z.Y.; Chai, S.P.; Zhu, P.W.; Mohamed, A.R. Development of a hybrid membrane through coupling of high selectivity zeolite T on ZIF-8 intermediate layer and its performance in carbon dioxide and methane gas separation. *Microporous Mesoporous Mater.* **2014**, *196*, 79–88.
127. Li, J.; Cao, W.; Mao, Y.; Ying, Y.; Sun, L.; Peng, X. Zinc hydroxide nanostrands: Unique precursors for synthesis of ZIF-8 thin membranes exhibiting high size-sieving ability for gas separation. *CrystEngComm* **2014**, *16*, 9788–9791.
128. Liu, Y.; Peng, Y.; Wang, N.; Li, Y.; Pan, J.H.; Yang, W.; Caro, J. Significantly enhanced separation using ZIF-8 membranes by partial conversion of calcined layered double hydroxide precursors. *ChemSusChem* **2015**, *8*, 3582–3586.
129. Wang, Y.; Jin, H.; Ma, Q.; Mo, K.; Mao, H.; Feldhoff, A.; Cao, X.; Li, Y.; Pan, F.; Jiang, Z. A MOF glass membrane for gas separation. *Angew. Chem.* **2020**, *132*, 4395–4399.

130. Cacho-Bailo, F.; Etxeberría-Benavides, M.; Karvan, O.; Téllez, C.; Coronas, J. Sequential amine functionalization inducing structural transition in an aldehyde-containing zeolitic imidazolate framework: Application to gas separation membranes. *CrystEngComm* **2017**, *19*, 1545–1554.
131. Mubashir, M.; Fong, Y.Y.; Leng, C.T.; Keong, L.K. Optimization of spinning parameters on the fabrication of NH_2-MIL-53(Al)/cellulose acetate (CA) hollow fiber mixed matrix membrane for CO_2 separation. *Sep. Purif. Technol.* **2019**, *215*, 32–43.
132. Meshkat, S.; Kaliaguine, S.; Rodrigue, D. Mixed matrix membranes based on amine and non-amine MIL-53(Al) in Pebax® MH-1657 for CO_2 separation. *Sep. Purif. Technol.* **2018**, *200*, 177–190.
133. Sabetghadam, A.; Liu, X.L.; Orsi, A.F.; Lozinska, M.M.; Johnson, T.; Jansen, K.M.B.; Wright, P.A.; Carta, M.; McKeown, N.B.; Kapteijn, F.; Gascon, J. Towards high performance metal–organic framework–microporous polymer mixed matrix membranes: Addressing compatibility and limiting aging by polymer doping. *Chem. Eur. J.* **2018**, *24*, 12796–12800.
134. Fan, Y.F.; Yu, H.Y.; Xu, S.; Shen, Q.C.; Ye, H.M.; Li, N.W. Zn(II)-modified imidazole containing polyimide/ZIF-8 mixed matrix membranes for gas separations. *J. Membr. Sci.* **2020**, *597*, 117775.
135. Meshkat, S.; Kaliaguine, S.; Rodrigue, D. Comparison between ZIF-67 and ZIF-8 in Pebax® MH-1657 mixed matrix membranes for CO_2 separation. *Sep. Purif. Technol.* **2020**, *235*, 116150.
136. Wang, Z.; Wang, D.; Zhang, S.; Hu, L.; Jin, J. Interfacial design of mixed matrix membranes for improved gas separation performance. *Adv. Mater.* **2016**, *28*, 3399–3405.
137. Nafisi, V.; Hagg, M.B. Development of dual layer of ZIF-8/PEBAX-2533 mixed matrix membrane for CO_2 capture. *J. Membr. Sci.* **2014**, *459*, 244–255.
138. Dong, L.; Chen, M.; Li, J.; Shi, D.; Dong, W.; Li, X.; Bai, Y. Metal-organic framework-graphene oxide composites: A facile method to highly improve the CO_2 separation performance of mixed matrix membranes. *J. Membr. Sci.* **2016**, *520*, 801–811.
139. Li, H.; Tuo, L.; Yang, K.; Jeong, H.K.; Dai, Y.; He, G.; Zhao, W. Simultaneous enhancement of mechanical properties and CO_2 selectivity of ZIF-8 mixed matrix membranes: Interfacial toughening effect of ionic liquid. *J. Membr. Sci.* **2016**, *511*, 130–142.
140. Jeazet, H.B.T.; Sorribas, S.; Román-Marín, J.M.; Zornoza, B.; Téllez, C.; Coronas, J. Increased selectivity in CO_2/CH_4 separation with mixed-matrix membranes of polysulfone and mixed-MOFs MIL-101(Cr) and ZIF-8. *Eur. J. Inorg. Chem.* **2016**, 4363–4367.
141. Xin, Q.P.; Ouyang, J.Y.; Liu, T.Y.; Li, Z.; Li, Z.; Liu, Y.C.; Wang, S.F.; Wu, H.; Jiang, Z.Y.; Gao, X.Z. Enhanced interfacial interaction and CO_2 separation performance of mixed matrix membrane by incorporating polyethylenimine-decorated metal–organic frameworks. *ACS Appl. Mater. Interfaces* **2015**, *7*, 1065–1077.
142. Japip, S.; Xiao, Y.; Chung, T.S. Particle-size effects on gas transport properties of 6FDA-Durene/ZIF-71 mixed matrix membranes. *Ind. Eng. Chem. Res.* **2016**, *55*, 9507–9517.
143. Hao, L.; Liao, K.S.; Chung, T.S. Photo-oxidative PIM-1 based mixed matrix membranes with superior gas separation performance. *J. Mater. Chem. A* **2015**, *3*, 17273–17281.
144. Ghalei, B.; Sakurai, K.; Kinoshita, Y.; Wakimoto, K.; Isfahani, A.P.; Song, Q.; Doitomi, K.; Furukawa, S.; Hirao, H.; Kusuda, H.; Kitagawa, S.; Sivaniah, E. Enhanced selectivity in mixed matrix membranes for CO_2 capture through efficient dispersion of amine-functionalized MOF nanoparticles. *Nat. Energy.* **2017**, *2*, 17086.
145. Yu, G.L.; Zou, X.Q.; Sun, L.; Liu, B.S.; Wang, Z.Y.; Zhang, P.P.; Zhu, G.S. Constructing connected paths between UiO-66 and PIM-1 to improve membrane CO_2 separation with crystal-like gas selectivity. *Adv. Mater.* **2019**, *31*, 1806853.
146. Venna, S.R.; Lartey, M.; Li, T.; Spore, A.; Kumar, S.; Nulwala, H.B.; Luebke, D.R.; Rosi, N.L.; Albenze, E. Fabrication of MMMs with improved gas separation properties using externally-functionalized MOF particles. *J. Mater. Chem. A* **2015**, *3*, 5014–5022.
147. Jiang, X.; Li, S.; He, S.; Bai, Y.; Shao, L. Interface manipulation of CO_2–philic composite membranes containing designed UiO-66 derivatives towards highly efficient CO_2 capture. *J. Mater. Chem. A* **2018**, *6*, 15064–15073.
148. Tien-Binh, N.; Vinh-Thang, H.; Chen, X.Y.; Rodrigue, D.; Kaliaguine, S. Crosslinked MOF-polymer to enhance gas separation of mixed matrix membranes. *J. Membr. Sci.* **2016**, *520*, 941–950.